Journal of Alloys and Compounds 516 (2012) 113–118

Contents lists available at SciVerse ScienceDirect

Journal of Alloys and Compounds

journal homepage: www.elsevier.com/locate/jallcom

Synthesis, characterization and transport properties of $Pr_{0.50}Ln_{0.50}BaCo_2O_{5+\delta}$ (Ln: Pr, Nd, Sm, Eu, Gd, Tb and Dy)

B. Rivas-Murias [a,*], J. Rivas [b], M.A. Señarís-Rodríguez [a]

[a] Departamento de Química Fundamental, Facultad de Ciencias, Universidad de A Coruña, 15701 A Coruña, Spain
[b] Departamento de Física Aplicada, Facultad de Física, Universidad de Santiago de Compostela, 15782 Santiago de Compostela, Spain

ARTICLE INFO

Article history:
Received 2 September 2011
Received in revised form
17 November 2011
Accepted 29 November 2011
Available online 8 December 2011

Keywords:
Cobalt oxides
Sol–gel synthesis
Transport properties
Power factor

ABSTRACT

In this work, we present the new compounds $Pr_{0.50}Ln_{0.50}BaCo_2O_{5+\delta}$ (Ln: Pr, Nd, Sm, Eu, Gd, Tb and Dy) that we have synthesized as pure phase polycrystalline materials by the Pechini method. Doping the A site with a second heavier lanthanide promotes smaller oxygen stoichiometry, providing an alternative way to modify the oxygen content of these Pr-cobalt oxides by means of changing the PrLn ratio. According to powder X-Ray diffraction the compounds display an average tetragonal structure. The presence of smaller Ln ions together with a smaller amount of oxygen gives rise to higher Seebeck coefficients, specially from PrEu to PrDy, and to a substantial increase of the resistivity below 200 K. As a result the highest power factor is displayed by the $Pr_{0.50}Eu_{0.50}BaCo_2O_{5.69}$ sample at ~125 K, PF_{max} ~0.154 μW K^{-2} cm^{-1}, value that is two orders of magnitude higher than that shown by the starting $PrBaCo_2O_{5.76}$ sample at the same temperature.

1. Introduction

Thermoelectric (TE) materials are attracting a lot of attention as an alternative for power generation from waste heat and for refrigeration [1,2]. Their performance can be evaluated using the dimensionless figure of merit (ZT) defined as $ZT = S^2\sigma\kappa^{-1}$, where S is the Seebeck coefficient of the material, σ its electrical conductivity, T is the absolute temperature, and κ its thermal conductivity. The product $S^2\sigma$ is related to electric power for thermoelectric generation and is called the power factor.

A good thermoelectric material should then possess a large power factor – that is, a high Seebeck coefficient together with a high electrical conductivity – and a relatively low thermal conductivity, requirements that are not easy to achieve due to the interrelationships among these three parameters. In general, σ increase leads to S decrease and κ increase.

Nowadays, the best thermoelectric performances are given by intermetallic compounds such as $(Bi, Sb)_2(Te,Se)_3$, filled skutterudites, etc. [3,4]. These compounds present relative high values of ZT, higher than 1. For a widespread application, the development of new thermoelectric materials with higher values of ZT and less harmful elements is desirable. In this context, ceramic oxide materials are receiving increased attention due to their added advantages, such as higher thermal stability, excellent oxidation resistance, lower cost and weaker toxicity.

In fact, several cobalt oxides have been identified as potential p- or n-type TE candidates, such as $NaCo_2O_4$ [5], $Ca_3Co_4O_9$ [6] and $CaMnO_3$ [7].

Another family that is arising interest is that of cobalt perovskites $Ln_{1-x}M_xCoO_{3-\delta}$ and related systems, as they display large Seebeck coefficients [8,9].

In this paper we focus on the related cobalt oxides $LnBaCo_2O_{5+\delta}$, that have recently received attention in view of the giant magnetoresistance displayed by some of its members [10,11]. These compounds present an oxygen-deficient perovskite-related 112-type structure ($a_p \times a_p \times 2a_p$, where a_p refers to the perovskite subcell) [12], that consists of double-pyramidal cobalt layers containing Ba^{2+} interspersed by lanthanide layers.

These $LnBaCo_2O_{5+\delta}$ materials can accommodate a large variation of oxygen content, between 5 and 6 ($0 \le \delta \le 1$) depending on the synthesis conditions [10,11,13,14] and the rare earth ion [10]. In this context, it has been observed that as the size of the rare earth decreases the oxygen content diminishes [10], resulting in changes in the coordination of the Co ions (pyramidal, octahedral) and in the formation of different polymorphs [10,14]. Thus, with larger (Pr) and smaller (Dy, Ho) rare-earths, the structures are tetragonal, while with intermediate-sized lanthanides (Sm, Eu Gd, Tb) they are orthorhombic [10,15]. Also, on reducing the oxygen content of Ln: Tb, the symmetry converts from orthorhombic to tetragonal whereas for Ln: Nd the opposite occurs [14,16].

* Corresponding author. Current address: Departamento de Química-Física y Centro Singular de Investigación en Química Biológica y Materiales Moleculares, Universidad de Santiago de Compostela, 15782 Santiago de Compostela, Spain. Tel.: +34 881815770; fax: +34 981595012.
E-mail addresses: beatriz.rivas@usc.es, beosky@yahoo.es (B. Rivas-Murias).

0925-8388/$ – see front matter © 2011 Elsevier B.V. All rights reserved.
doi:10.1016/j.jallcom.2011.11.146

Simultaneously, the Co mean valence (that can vary from 2.5+ for $\delta = 0$ to 3.5+ for $\delta = 1$) and spin state also change, factors that will directly affect the magnetic and transport properties of these compounds.

And even if the impact of these variables on their magnetic behavior has been analyzed more in depth [10,11,13,17] there have been fewer systematic studies on their influence on the transport properties, aspect that is of great interest in the search for new thermoelectrics. In that context we have recently reported large differences on the power factor of $PrBaCo_2O_{5+\delta}$ samples by changing their oxygen content and degree of particle sintering, through adequate thermal treatments under argon/oxygen flow or by electrochemical oxidation/reduction [18].

In this work, we focus on an alternative method to modify the oxygen content of these $PrBaCo_2O_{5+\delta}$ materials with the aim of optimizing their thermoelectric behavior. It consists in carrying out a partial (50%) substitution of the Pr cation at the A site for other smaller lanthanide cations (Ln: Nd, Sm, Eu, Gd, Tb and Dy). To the best of our knowledge such double doping at the A site has not been previously reported for these cobalt systems so that the obtained compounds would be new members of the $LnBaCo_2O_{5+\delta}$ series. And we have investigated the influence of such rare earth substitution on the structure, electrical resistivity, thermopower and power factor of the obtained materials.

2. Experimental

The compounds $Pr_{0.50}Ln_{0.50}BaCo_2O_{5+\delta}$ (Ln: Pr, Nd, Sm, Eu, Gd, Tb, Dy; hereafter labeled Pr, PrNd, PrSm, PrEu, PrGd, PrTb, PrDy, respectively) were prepared by the Pechini method [19]. For this purpose, adequate amounts of Pr_6O_{11}, Tb_4O_7 and Ln_2O_3 (Ln: Nd, Sm, Eu, Gd, Dy) were first converted into the corresponding nitrate by dissolution in HNO_3 (30%). These were then added to a 1 M citric acid aqueous solution, in which stoichiometric amounts of $BaCO_3$ (99+%, Aldrich) and $Co(NO_3)_2{\cdot}6H_2O$ (98+%, Aldrich) were also dissolved. After diluting the so-obtained solution, ethylene glycol was carefully added in a proportion 10% v/v.

After heating and evaporating the resulting solution at 110 °C, the obtained brown gel was decomposed by heating at 400 °C/1 h.

The obtained powders were pressed into pellets and heated in air at different temperatures (600 °C, 700 °C, 800 °C and 950 °C) with intermediate grindings to obtain single-phase and homogeneous samples. Finally, the last treatment was at 1000 °C for 5 h followed by a slow cool to room temperature (0.7 °C/min).

The samples were characterized at room temperature by powder X-ray diffraction (PXRD) using a Siemens D-5000 diffractometer, a theta/2-theta diffraction instrument operating in reflection geometry using Cu (K_α) = 1.5418 Å radiation. Rietveld analysis of the powder X-ray diffraction data was carried out using the Rietica software suite [20].

The morphology and particle size of the polycrystalline samples were studied by scanning electron microscopy (SEM), using a Jeol 6400 microscope.

Iodometric titrations were carried out to analyze the oxygen content of the samples. For this purpose, the samples were dissolved in acidified KI solutions (HCl ~ 5 M), and the I_2 generated was titrated against a thiosulphate solution. All the process was carried out under an argon atmosphere and repeated twice to confirm the accuracy of the results.

The electrical resistivity, ρ, was measured as a function of temperature in the range $78 \leq T(K) \leq 300$ using a dc four-probe method. Seebeck coefficients of pressed pellets were measured in the temperature range $85 \leq T(K) \leq 450$ in a homemade device.

Finally, the power factor of these samples (defined as $PF = S^2/\rho$) was calculated from the obtained electrical resistivity and Seebeck coefficient data.

3. Results and discussion

3.1. Sample characterization

According to the powder X-ray diffraction results, single-phase crystalline materials $Pr_{0.50}Ln_{0.50}BaCo_2O_{5+\delta}$ have been obtained for Ln: Pr, Nd, Sm, Eu, Gd, Tb and Dy (Fig. 1), enlarging the family of $LnBaCo_2O_{5+\delta}$ compounds.

These polycrystalline materials consist of not completely homogeneous particles with average diameter 1–2 μm, as shown by SEM micrographs (see Fig. 2). The particle size of these samples decreases slightly as the Ln cation gets smaller from Pr- (1–2 μm) down to the Sm-sample (~1 μm). In those with intermediate lanthanides, PrEu, PrGd and PrTb, small particles (~1 μm) are seen to coexist with higher aggregates (~3 μm), formed by the coalescence of small particles. Finally the PrDy sample presents the smallest particles (0.5–0.8 μm).

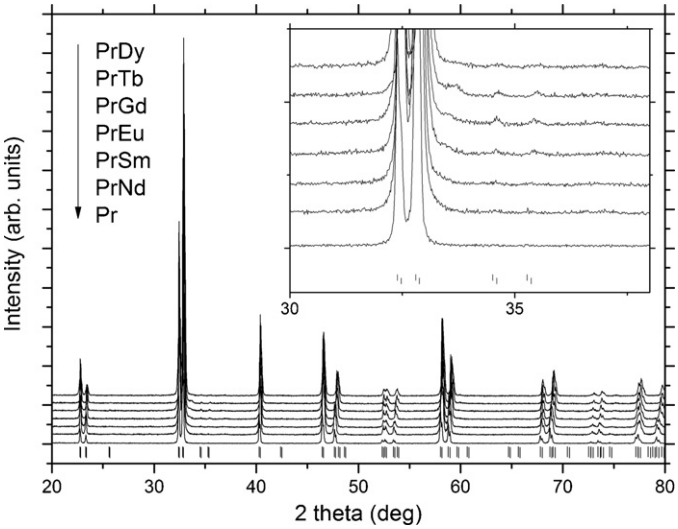

Fig. 1. PXRD patterns of $Pr_{0.50}Ln_{0.50}BaCo_2O_{5+\delta}$ samples (Ln: Pr–Dy) and corresponding Rietveld refinements. The lower tick marks indicate peak positions of P4/mmm space group. *Inset*: Detail between 30 and 38°.

As for their oxygen content, the iodometric titrations indicate that the as-prepared samples are oxygen-deficient, including the starting Pr-sample. Interestingly enough, in the as-prepared samples the oxygen content decreases smoothly upon doping with heavier lanthanides from 5.76 ± 0.02 per unit formula for Pr down to 5.62 ± 0.02 for PrTb and PrDy (see Table 1). Such trend is in agreement with earlier reports on the variation of the oxygen content of $LnBaCoO_2O_{5+\delta}$ compounds containing a single rare earth [10,14,21], even if the presence of 50% Pr reduces the decrease in oxygen content that never gets as low as for example in the case of the $HoBaCoO_2O_{5+\delta}$ compound ($\delta = 0{\cdot}25$) [14].

The X-ray diffraction patterns of all these samples can be indexed on the basis of a tetragonal structure with cell parameters $a_c \times a_c \times 2a_c$ (space group P4/mmm) (see Table 1). As no orthorhombic distortion is observed by laboratory X-ray diffraction (lack of peak splitting at ~22.7° and 46.5°), not even in the samples with higher oxygen deficiency, one could be tempted to interpret this result as an inhomogeneous distribution of the oxygen vacancies in the LnO_x planes [11]. Nevertheless, this point can only be unambiguously established by neutron diffraction or synchrotron powder diffraction, as conventional PXRD data do not really allow to determine if the cell parameters are doubled or not and how is the distribution of the oxygen vacancies.

Therefore, the local structure in these $Pr_{0.50}Ln_{0.50}BaCo_2O_{5+\delta}$ samples can be in fact much more complex than the average situation detected by PXRD, as it occurs in other $LnBaCo_2O_{5+\delta}$ systems [10,22], where the presence of superstructures in the electron diffraction patterns are also common [14].

The range of oxygen content for the presence of the tetragonal phase in these $Pr_{0.50}Ln_{0.50}BaCo_2O_{5+\delta}$ compounds compares well with that reported for the $PrBaCo_2O_{5+\delta}$ [18] and $NdBaCo_2O_{5+\delta}$ systems [14], even if it is larger than that found in the $GdBaCo_2O_{5+\delta}$ system [22], in which an intrinsic mixture of tetragonal and orthorhombic phase is already detected at the lower edge of the compositional range of $\delta > 0.60$.

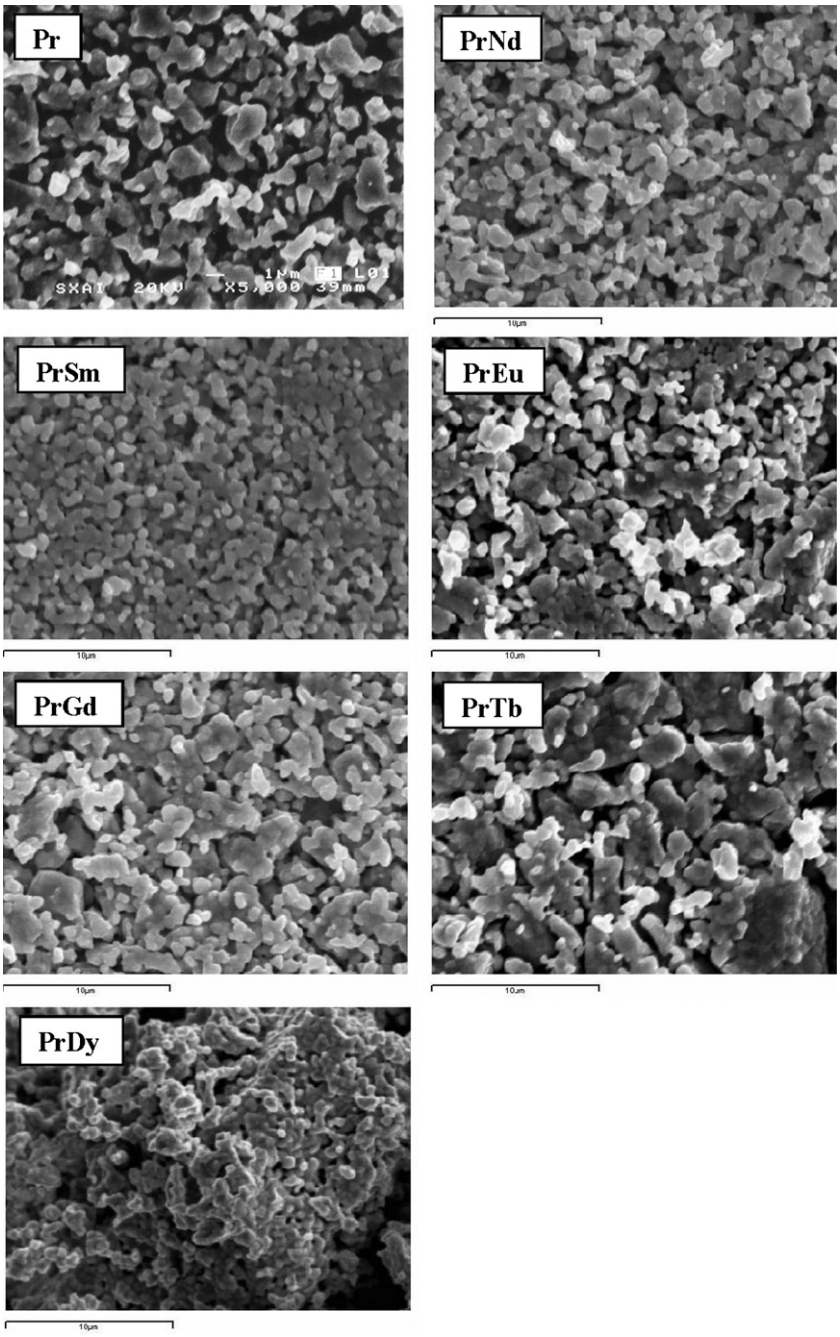

Fig. 2. SEM micrographs of $Pr_{0.50}Ln_{0.50}BaCo_2O_{5+\delta}$ samples.

As for the variation of the lattice parameters along this series, both a and c slowly diminish as the dopant changes from Pr to PrDy and the oxygen deficiency increases, see Table 1. Such decrease is slightly more important for the c axis, even if it is not as pronounced as the behavior found in $LnBaCo_2O_{5+\delta}$ samples (c axis changes from ~7.63 to ~7.50 Å, for Ln = Pr and Dy, respectively) [10,14]. As a result, in these $Pr_{0.50}Ln_{0.50}BaCo_2O_{5+\delta}$ compounds the cell volume is seen to decrease as the dopant Ln ions change from Nd to Dy, as it also occurs in the equivalent compounds that contain a single rare-earth ion [10,14]. Such decrease correlates with the decrease

Table 1
Oxygen content and cell parameters for the different $Pr_{0.50}Ln_{0.50}BaCo_2O_{5+\delta}$ samples.

Sample	Pr	PrNd	PrSm	PrEu	PrGd	PrTb	PrDy
Oxygen content	5.76	5.76	5.74	5.69	5.64	5.62	5.62
Cell parameters							
a (Å)	3.9069 (1)	3.8986 (1)	3.8984 (1)	3.8981 (1)	3.8964 (1)	3.8945 (1)	3.8917 (1)
c (Å)	7.6290 (2)	7.6241 (1)	7.6189 (2)	7.5974 (2)	7.5889 (2)	7.5794 (2)	7.5744 (2)
Mean A-site radius (Å)	2.649	2.641	2.625	2.619	2.613	2.607	2.601

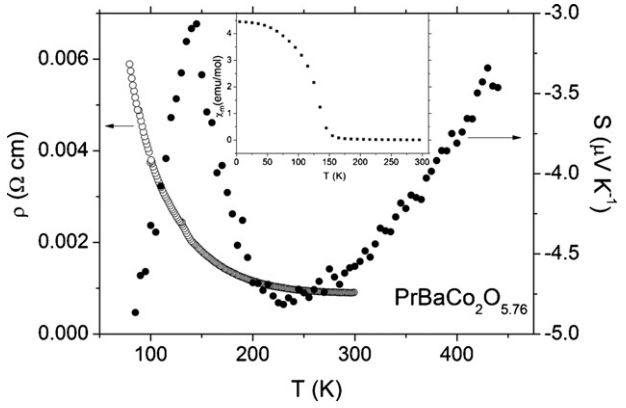

Fig. 3. Temperature dependence of the electrical resistivity and thermoelectric power for the starting $PrBaCo_2O_{5.76}$ sample (Pr). *Inset*: FC molar magnetic susceptibility under 1 kOe.

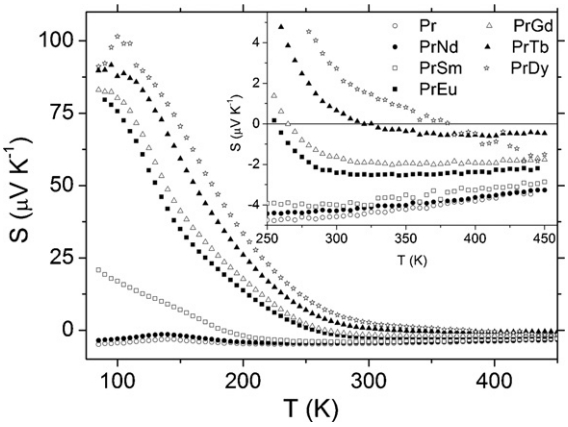

Fig. 5. Temperature dependence of the thermoelectric power for $Pr_{0.50}Ln_{0.50}BaCo_2O_{5+\delta}$ compounds (Ln: Pr–Dy). *Inset*: Detail of the thermoelectric power at high temperature.

in the mean A-site radius, $\bar{r}_A$, which is calculated using the tabulated values for atoms in ninefold coordination (see Table 1) [23]. This behavior shows deviations from a merely linear function as not only this parameter is changing along the series but also the oxygen content of the samples.

3.2. Transport properties

The starting $PrBaCo_2O_{5.76}$ sample shows an almost metallic behavior for $T > 200$ K, with a small resistivity that is almost constant above that temperature ($\rho \sim 1$ mΩ cm) and a small negative thermopower that increases linearly with temperature (Fig. 3). At lower temperatures the resistivity is seen to increase with descending temperatures while the thermopower goes through a maximum centered at 140 K. Above this temperature the ferromagnetic ordering takes place in the Co—O sublattice (see inset Fig. 3). These results are in agreement with those reported in the literature [11]. Upon doping with heavier lanthanide ions the first general remark is that the resistivity of the samples is seen to rapidly increase below 200 K, specially those from PrEu to PrDy. Such resistivity values then almost converge to a same value at higher temperatures (Fig. 4). The increase of the resistivity can be explained by the fact that the doping with heavier and smaller lanthanide ions weakens the Co—O interactions (small Co—O distances and angles) getting narrower bandwidths, which favor localized states.

As for their thermopower (Fig. 5), while that of the PrNd sample (high cation size) is similar to the starting Pr-sample, doping with Eu, Gd, Tb and Dy (small size) gives rise to a marked change in the Seebeck coefficient at low temperatures: it becomes positive and much higher (80–90 μV K^{-1} at 100 K) to then decrease as temperature gets higher and become negative. Meanwhile, the PrSm sample (intermediate size) shows an intermediate behavior.

Consequently, in the samples from PrSm to PrDy, and contrary to the case of the Pr and PrNd samples, the predominant charge carriers are holes below ~180 K for PrSm sample and ~380 K for PrDy sample (see the critical temperature for the other compounds in inset Fig. 5). Their number decrease from PrSm to PrDy as the Seebeck coefficient values get positive and with higher absolute values.

Taking into account that from PrEu to PrDy (small Ln cation size) a $\alpha \sim 1/T$ dependence is observed for $\sim 110 < T(K) < 250$ (Fig. 6), we assume that they behave as band gap materials with a fixed activation energy $E_g \ggg kT$ for the creation of mobile holes and trapped electrons.

If the mobile holes are non-adiabatic small polarons, the energy gap (E_g) can be calculated from the Seebeck data as [24–26]

$$\alpha - \alpha_0 \approx \frac{-k_B}{e} \ln\left(\frac{1-p}{p}\right) \approx \frac{E_g}{2eT} \quad (1)$$

where α is the Seebeck coefficient, k_B is the Boltzmann constant, e is the electron charge and p is the charge carrier concentration.

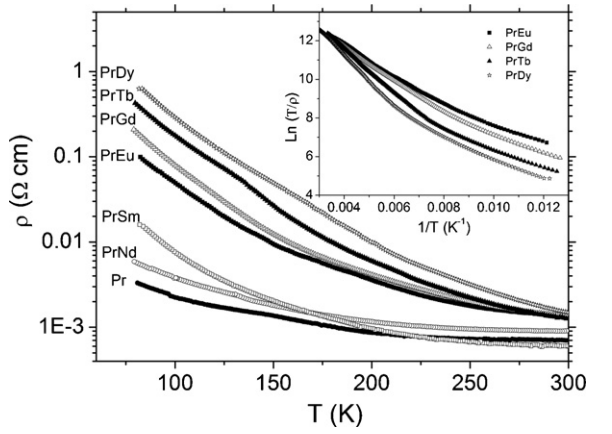

Fig. 4. Temperature dependence of the electrical resistivity for $Pr_{0.50}Ln_{0.50}BaCo_2O_{5+\delta}$ compounds (Ln: Pr–Dy). *Inset*: Fitting to small polaron behavior of the PrEu, PrGd, PrTb and PrDy samples.

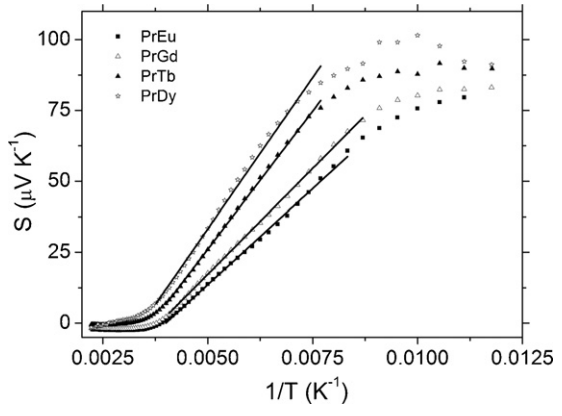

Fig. 6. Thermoelectric power versus $1/T$ for $Pr_{0.50}Ln_{0.50}BaCo_2O_{5+\delta}$ compounds (Ln: Pr–Dy).

Table 2
Gap energy, motional enthalpy and activation energy for the different $Pr_{0.50}Ln_{0.50}BaCo_2O_{5+\delta}$ samples.

Sample	PrEu	PrGd	PrTb	PrDy
E_g (meV)	27	30	39	43
AH_m (meV)	56	59	76	94
E_a (meV)	69	74	96	116

To obtain the motional enthalpy of the small-polaron holes with mobility

$$\mu_p = \frac{eD_0}{k_B T} \exp\left(\frac{-AG_m}{k_B T}\right) \quad (2)$$

we use the conductivity expression defined by

$$\sigma = pe\mu_p \approx T^{-1} \exp\left(\frac{-E_a}{k_B T}\right) \quad (3)$$

with $E_a = \Delta H_m + (E_g/2)$ and $\Delta G_m = \Delta H_m - T\Delta S_m$

For small polarons, the mobile hole density is $p = p_0 \exp(-E_g/2\,k_B T)$ with p_0 independent of temperature and

$$\ln\left(\frac{T}{\rho}\right) = \text{const} - \left(\frac{E_a}{k_B T}\right) \quad (4)$$

where ρ is the measured resistivity.

From Eqs. (1) and (4) and from the corresponding fittings, that contrary to the case of other cobaltite systems [18,27] are reasonably good (see inset in Figs. 4 and 6), we obtain E_g and ΔH_m values which are summarized in Table 2. Such values, that in all cases are small, reveal that upon doping with heavier lanthanides the motional enthalpy of the p-type charge carriers, that is the main contribution to the activation energy, increases.

Such a result can be rationalized taking into account both the effect of the A cations on the electronic structure of the cobaltites and the effect of a higher oxygen deficiency.

In this context, the presence of smaller and more acidic (higher charge/radius ratio) Ln ions will weaken the Co—O interactions resulting in narrower bandwidths, smaller ferromagnetic interactions and lower spin states [28], thus favoring more localized states. A smaller oxygen content accompanying the presence of heavier Ln ions will also contribute in the same direction (to a higher resistivity): smaller hole doping in the Co—O sublattice (smaller amount of formally Co^{4+} ions, that diminishes from $PrBaCo_2O_{5.76}$ to $Pr_{0.50}Dy_{0.50}BaCo_2O_{5.62}$) as well as a certain disorder associated with the presence of oxygen vacancies.

From the obtained thermopower and resistivity data we have calculated the power factor (PF) of these samples (Fig. 7), that evaluates their thermoelectric performance. As it can be seen, it increases from Pr to PrEu to then slightly decrease up to PrDy.

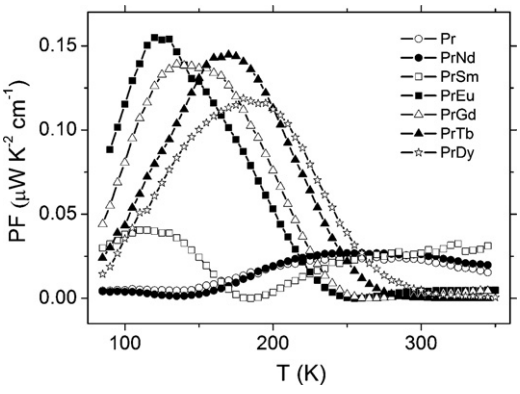

Fig. 7. Power factor as a function of temperature for $Pr_{0.50}Ln_{0.50}BaCo_2O_{5+\delta}$ compounds (Ln: Pr–Dy).

The relative high values displayed by PrEu, PrGd, PrTb and PrDy at low temperatures ($PF_{max} \sim 0.154\,\mu W\,K^{-2}\,cm^{-1}$ at ~ 125 K for $Pr_{0.50}Eu_{0.50}BaCo_2O_{5.69}$) as compared to that shown by the starting $PrBaCo_2O_{5.76}$ sample ($PF \sim 0.005\,\mu W\,K^{-2}\,cm^{-1}$ at ~ 125 K) result from an increased Seebeck coefficient at low and intermediate temperatures that overcomes the higher resistivity displayed by these samples.

It should be noted that a similar tendency has been recently found in $PrBaCo_2O_{5+x}$ system [18] as the oxygen content is reduced from 5.76 to 5.54.

The temperature dependence of the power factor can be divided into different behaviors. Firstly, smaller A-cation size presents a maximum in the range 120–200 K, i.e., the PrEu, PrGd, PrTb and PrDy samples. In this range, the Seebeck coefficient overcomes the resistivity increase of the samples. Secondly, higher A-cation size shows a maximum value at ~260 K, as well the Seebeck coefficient as the resistivity present small values. Finally, the intermediate A-cation size (the PrSm sample) displays an intermediate behavior, showing a maximum and a constant value at low and high temperatures, respectively (Fig. 7).

If we now compare the power factor of these lanthanide doped samples with undoped samples but with similar oxygen content (see Ref. [18]), we observe that the PrGd sample ($\delta = 0.64$) shows twice smaller values of the power factor in comparison with the corresponding $PrBaCo_2O_{5.64}$ Ar-annealed sample. This difference can be explained by the mixture of orthorhombic and tetragonal phases found in the latter case. The orthorhombic phase probably shows a lower hole doping and dominates the thermopower behavior at low temperatures, giving rise to higher α values than expected.

On the other hand, in the case of the PrSm sample ($\delta = 0.74$), the values of the power factor are similar to those of the $PrBaCo_2O_{5.72}$ Ar-annealed sample.

The power factor enhancement observed in this work is not as important as that observed in Ref. [18] but this approach of improving the TE response with the Ln cation substitution should be an interesting alternative way to the more tedious and complicated treatments under oxidizing and reducing atmospheres. Furthermore, more studies to improve the intergrain electrical conductivity of these samples are desirable to optimize their thermoelectric response.

4. Conclusions

In summary, we have prepared the new compounds $Pr_{0.50}Ln_{0.50}BaCo_2O_{5+\delta}$ (Ln: Pr, Nd, Sm, Eu, Gd, Tb and Dy) as pure phase materials by the Pechini method and we have characterized them chemically and by powder X-ray diffraction. It is observed that doping the A-site with a second heavier lanthanide promotes smaller oxygen content, providing an alternative way to modify their oxygen content. According to powder X-ray diffraction all these compounds, even those with higher oxygen deficiency, display an average tetragonal structure with $a = b \cong a_c$ and $c \cong 2a_c$ (space group P4/mmm), whose cell parameters diminish as the size of the doping lanthanide size decreases.

The presence of smaller Ln ions together with a smaller amount of oxygen gives rise to higher Seebeck coefficients, specially from PrEu to PrDy. As for the resistivity, the doping with heavier lanthanide ions induces an increase of the resistivity below 200 K. As a result, the maximum power factor is shown by $Pr_{0.50}Eu_{0.50}BaCo_2O_{5.69}$ at ~ 125 K, $PF_{max} \sim 0.154\,\mu W\,K^{-2}\,cm^{-1}$, value that is two orders of magnitude higher than that obtained for the starting $PrBaCo_2O_{5.76}$ compound. This strategy of modifying the oxygen content, structural, and electronic characteristics of these Co-compounds by introducing two different rare earth ions

at the A-sites is thus an alternative approach to try to optimize the thermoelectric response of these materials.

Acknowledgments

M.A.S.R. is grateful for financial support from Ministerio de Ciencia e Innovación MICINN (Spain) under project FEDER MAT2010-21342-C02-01 and from Xunta de Galicia under project PGIDIT10PXB103272PR.

References

[1] F.J. DiSalvo, Science 285 (1999) 703.
[2] L.E. Bell, Science 321 (2008) 1457.
[3] G. Mahan, B. Sales, J. Sharp, Phys. Today 50 (1997) 42.
[4] D.M. Rowe, CRC Handbook of Thermoelectrics, CRC Press, Boca Raton, FL, 1995.
[5] I. Terasaki, Y. Sasago, K. Uchinokura, Phys. Rev. B 56 (1997) R12685.
[6] T. Yin, D. Liu, Y. Ou, F. Ma, S. Xie, J.-F. Li, J. Li, J. Phys. Chem. C 114 (2010) 10061.
[7] Y. Wang, Y. Sui, H. Fan, X. Wang, Y. Su, X. Liu, Chem. Mater. 21 (2009) 4653.
[8] J. Androulakis, P. Migiakis, J. Giapintzakis, Appl. Phys. Lett. 84 (2004) 1099.
[9] T. He, J. Chen, T.G. Calvarese, M.A. Subramanian, Solid State Sci. 8 (2006) 467.
[10] A. Maignan, C. Martin, D. Pelloquin, N. Nguyen, B. Raveau, J. Solid State Chem. 142 (1999) 247.
[11] C. Frontera, A. Caneiro, A.E. Carrillo, J. Oró-Solé, J.L. García-Muñoz, Chem. Mater. 17 (2005) 5439.
[12] L. Er-Rakho, C. Michel, Ph Lacorre, B. Raveau, J. Solid State Chem. 73 (1988) 531.
[13] S. Streule, A. Podlesnyak, J. Mesot, M. Medarde, K. Conder, E. Pomjakushina, E. Mitberg, V. Kozhevnikov, J. Phys.: Condens. Matter 17 (2005) 3317.
[14] P.S. Anderson, C.A. Kirk, J. Knudsen, I.M. Reaney, A.R. West, Solid State Sci. 7 (2005) 1149.
[15] I.O. Troyanchuk, N.V. Kasper, D.D. Khalyavin, H. Szymczak, R. Szymczak, M. Baran, Phys. Rev. B 58 (1998) 2418.
[16] I.O. Troyanchuk, N.V. Kasper, D.D. Khalyavin, A.N. Chobot, G.M. Chobot, H. Szymczak, J. Phys.: Condens. Matter 10 (1998) 6381.
[17] T.V. Aksenova, L.Yu. Gavrilova, A.A. Yaremchenko, V.A. Cherepanov, V.V. Kharton, Mater. Res. Bull. 45 (2010) 1288.
[18] B. Rivas-Murias, M. Sánchez-Andújar, J. Rivas, M.A. Señarís-Rodríguez, J. Alloys Compd. 509 (2011) 5250.
[19] F. Licci, T. Besagni, L. Rinaldi, European Patent, Application number 85860253-2.
[20] C.J. Howard, B.A. Hunter, Rietica: A Computer Program for Rietveld Analysis of X-ray and Neutron Powder Diffraction Patterns, Australian Nuclear Science and Technology (Organization Lucas Heights Research Laboratories), 1998.
[21] T. Dasgupta, S. Sumithra, A.M. Umarji, Bull. Mater. Sci. 31 (2008) 859.
[22] A.A. Taskin, A.N. Lavrov, Y. Ando, Phys. Rev. B 71 (2005) 134414.
[23] R.D. Shannon, Acta Cryst. A 32 (1976) 751.
[24] N.F. Mott, Conduction in Non-Crystalline Materials, Oxford University Press, New York, 1993.
[25] D.K.C. MacDonald, Thermoelectricity: An Introduction to the Principles, John Wiley & Sons, New York, 1962.
[26] M.A. Señarís-Rodríguez, J.B. Goodenough, J. Solid State Chem. 116 (1995) 224.
[27] A.K. Kundu, B. Raveau, V. Caignaert, E.-L. Rautama, V. Pralong, J. Phys.: Condens. Matter 21 (2009) 056007.
[28] C. Rey-Cabezudo, M. Sánchez-Andujar, J. Mira, A. Fondado, J. Rivas, M.A. Señarís-Rodríguez, Chem. Mater. 14 (2002) 493.